UCLA
COMPUTATIONAL AND APPLIED MATHEMATICS

On the Active Control of the Wake Past a Plate with a Suction Point on the Downstream Wall

L. Cortelezzi

April 1995

CAM Report 95-21

Department of Mathematics
University of California, Los Angeles
Los Angeles, CA. 90024-1555

On the active control of the wake past a plate with a suction point on the downstream wall.

by L. CORTELEZZI*

April 19, 1995

Abstract

Active circulation control of the two-dimensional unsteady separated flow past a plate with a suction point on the downstream wall is considered. The rolling-up of the separated shear-layer is modelled by a pair of point vortices whose time-dependent circulation is predicted by an unsteady Kutta condition. A nonlinear controller able to confine the wake to a single vortex pair of constant circulation is derived in closed-form for any free-stream condition. Dynamical system analysis is used to explore the performance of the controlled system. Finally, the control strategy is applied to three different classes of unsteady flows and the results are discussed.

*Department of Mathematics, University of California, Los Angeles, California 90024-1555, U.S.A. E-mail: crtlz@math.ucla.edu

1 Introduction

Active control of unsteady separated fluid flows is attracting wide interest in both the fluid mechanics and control communities because of the many potential engineering applications. See Gad-el-Hak & Bushnell (1991) for a discussion and references. Drag reduction, lift enhancement, noise and vibration control, mixing improvement, etc. are some of the many problems where active control of flows past bluff bodies finds natural applications.

The problem of actively controlling an unsteady fluid flow is in general nonlinear. Since the control of nonlinear systems remains a research topic, there is no general framework to obtain a desired controller. However, it is well known that the model chosen to represent the plant is of crucial importance in the derivation of the controller. A very complex and detailed model, the full Navier-Stokes equations for example, might generate an overly complex controller or might make the derivation of the controller impossible. On the other hand, an over-simplified or linear model facilitates the derivation of the controller but might generate a controller unable to achieve the desired control objective. A reasonable compromise is a reduced model able to capture the dynamic features of the flow that one wants to control. See Cao and Aubry 1993, Rajaee *et al.* 1994, Cortelezzi *et al.* 1994. Typically, the reduced model is a low-dimensional nonlinear system governed by a set of ordinary differential equations, while the real flow has infinite dimensions. An advantage of working with a reduced model is that one can use dynamical system analysis to investigate the problem. Analysis of the phase space of the reduced system provides information about fixed points, limit cycles, bifurcation points, etc., characteristic of the flow under consideration and consequently provides information about effectiveness and robustness of the controller. Another advantage of model reduction is the potential for producing fast numerical algorithms which are essential for controlling a real flow.

Before attempting to control a laboratory flow one should take the intermediate step of controlling the same class of flows simulated by a more sophisticated CFD (Computational Fluid Dynamics) code. The application of the controller derived for the reduced model to a complex model should be successful if the two models are dynamically equivalent; i.e., if the phase spaces of the two models are topologically equivalent. The equivalence of the two models can be investigated via dynamical system and time series analysis. There are many advantages in controlling a flow simulated by another CFD code. All the flow quantities necessary to feedback to the controller can be easily measured. The action of the controller is automatically synchronized with the evolution of the flow because both algorithms run in virtual time. Furthermore, the controller can be tested on gradually more complex flows. For example, if the controller were derived for an inviscid model, then it could be applied to the same flow when the fluid is slightly viscous. In general the controller has to be made robust with respect to the perturbations introduced by the new environment, e.g., viscosity, three-dimensionality, background noise (see Doyle *et al.* 1992, Fan *et al.* 1991). Only an iteration process might produce a controller able to handle the flow simulated by the Navier-Stokes equations. Finally, the control of a laboratory flow can be attempted when the controller

generated by this chain of refinements is robust enough to perform in the presence of the unmodeled and unpredictable uncertainties affecting the real system and is fast enough to control the flow in real-time.

Recently, efforts to modify certain features of the wake behind bluff and slender bodies, such as reduction or magnification of the wake thickness (Tokumaru & Dimotakis 1991), wake stabilization (Roussopoulos 1993), vortex cancelation (Koochesfahani & Dimotakis 1988), pattern reproduction (Ongoren & Rockwell 1988*a*, *b*, Gopalkrishnan *et al.* 1994), and lift enhancement (Rossow 1977, Slomski & Coleman 1993) have been successful. In all these investigations the free-stream velocity was kept constant and quasi-steady results were achieved usually by moving the body or the actuator with a frequency scaled by the shedding frequency. In a more general situation in which the free-stream velocity is time dependent this approach is generally not sufficient to control the flow and a nonlinear control strategy is necessary.

The present study investigates the active control of the wake past a plate perpendicular to an unsteady fluid flow. In Section 2, following our previous work (see Cortelezzi 1995), we model the unsteady separation from the tips of a flat plate by means of a pair of point vortices whose time-dependent circulation is predicted by an unsteady Kutta condition. The problem is further simplified by imposing wake symmetry. The motion of the vortex pair is determined by a nonlinear ordinary differential equation first proposed by Brown and Michael in 1954. A suitable vortex shedding mechanism is also introduced to allow the simulation of flows involving multiple vortices. This reduced model is able to capture the main features of the flow and, for example, is quite accurate for power-law starting flows (see Cortelezzi 1995).

In Section 3, we consider as a control actuator a suction point placed on the downstream wall of the plate. The control objective is to confine the wake to a single vortex pair of constant circulation. We show that suction is a very efficient means to control the production of circulation. Thanks to the simplicity of the model we obtain for any time-dependent free-stream velocity the analytical closed-form solution of the controller; i.e., the predicted suction necessary to inhibit the production of circulation when a vortex pair is present in the flow.

In Section 4, we perform an analysis of dynamical system type to characterize the performance of the controller. When the free-stream is constant, we show the existence of fixed points for the unperturbed system and compute the locus of the fixed points. There is a critical value for the circulation associated with the vortex pair above which one can find two pairs of fixed points: a pair of stable nodes and a pair of saddle points farther downstream. The circulation plays the role of a bifurcation parameter and the vector field undergoes a saddle-node bifurcation when the circulation is near its critical value. The analysis of the phase space shows the existence of a controllable region between the plate and the stable manifolds of the saddle points. When the free-stream velocity oscillates periodically about a unit mean, we compute the Poincaré section to characterize the perturbed system. We show the topological equivalence between the Poincaré section and the phase space of the unperturbed system. The stable node of the Poincaré section represents a limit cycle while the saddle point represents an unsteady periodic orbit.

In Section 5, we present the results of three simulations. The first two simulations document the ability of the controller to drive the vortex pair to the stable nodes when the free-stream ve-

locity is constant or to a limit cycle when the free-stream velocity oscillates periodically. The third simulation documents the performance of the controller when the free-stream velocity oscillates pseudo-randomly.

2 Mathematical formulation

In this section we introduce a mathematical model of the two-dimensional unsteady separation from the tips of a finite plate with a suction point of strength s at the center of the downstream wall. Let us assume that the regions of vorticity that separate from the boundary layer and are convected away are thin enough to justify a description by means of a vortex sheet. The consequent stretching and rolling up of the vortex sheet, due to the unsteadiness of the flow, suggests a more coarse description via point vortices. The vortex sheet is not completely lost. It is assumed to be of negligible circulation which connects the feeding point to a point vortex of variable strength which is able to satisfy an unsteady Kutta condition. The mathematical representation of the feeding vortex sheet is simply the branch cut due to the logarithmic singularity representing the vortex. All the other vortices in the wake are represented by point vortices of fixed circulation.

We choose, for simplicity, a frame of reference fixed to the plate so that the body can be identified with the segment $[-2ia, 2ia]$ and the suction point s coincides with the point $(0^+, 0)$. Then, the flow of an incompressible irrotational fluid about such a body can be analyzed via conformal mapping. Using the Joukowski transformation

$$z = \zeta - \frac{a^2}{\zeta}, \tag{1}$$

we map the finite plate of length $L = 4a$ in the z-plane onto the circle of radius a in the ζ-plane (see Figure 1), preserving the characteristic of the flow at infinity.

To make the problem dimensionless we have to define a characteristic length and time scale. For this purpose we write the free-stream velocity as follows:

$$U(t) = U_\infty + u(t), \tag{2}$$

where U_∞ is the unperturbed free-stream velocity and $u(t)$ is the time dependent component. If we choose the circle radius as characteristic length and a/U_∞ as characteristic time of the problem then we can define the following dimensionless quantities:

$$\begin{aligned} z^* &= \frac{z}{a}, & \zeta^* &= \frac{\zeta}{a}, & a^* &= 1, & t^* &= \frac{U_\infty t}{a}, \\ U^* &= \frac{U}{U_\infty} = 1 + \epsilon_U, & \Gamma^* &= \frac{\Gamma}{U_\infty a}, & s^* &= \frac{s}{U_\infty a}. \end{aligned} \tag{3}$$

where Γ is the circulation. Note that $\epsilon_U = u/U_\infty$ contains the unsteadiness of the free-stream velocity and is not necessarily small with respect to unity. From this point on, we continue the mathematical formulation of the problem using dimensionless variables, where the stars are omitted for convenience.

There is experimental evidence (Lisosky 1993, private communication) that the near wake is nearly two dimensional and symmetric about the x-axis if the plate moves with a non-zero acceleration. Under these circumstances the problem can be simplified by imposing symmetry with respect to the real axis, i.e., by requiring that the vortices have equal and opposite circulation, Γ_n and $-\Gamma_n$, and are located in complex conjugate positions, ζ_n and $\bar{\zeta}_n$, respectively. Since the velocity field has to satisfy Laplace's equation and the boundary condition in the mapped plane can be treated using the circle theorem, we can build the complex potential F by superimposing basic flows. Thus, the complex velocity field $w = dF/d\zeta$ has the form:

$$\begin{aligned} w(\zeta,t) = U\left(1-\frac{1}{\zeta^2}\right) + \frac{i\Gamma_1}{2\pi}\left(\frac{1}{\zeta-\zeta_1} + \frac{\bar{\zeta}_1}{1-\zeta\bar{\zeta}_1} - \frac{1}{\zeta-\bar{\zeta}_1} - \frac{\zeta_1}{1-\zeta\zeta_1}\right) \\ + \sum_{n=2}^{N} \frac{i\Gamma_n}{2\pi}\left(\frac{1}{\zeta-\zeta_n} + \frac{\bar{\zeta}_n}{1-\zeta\bar{\zeta}_n} - \frac{1}{\zeta-\bar{\zeta}_n} - \frac{\zeta_n}{1-\zeta\zeta_n}\right) - s\frac{\zeta+1}{\zeta(\zeta-1)}. \end{aligned} \tag{4}$$

Note that for convenience we take the circulation to be positive when in clockwise sense, contrary to the usual convention. Note also that the singularity on the back face of the plate behaves as a sink when $s > 0$ and as a source otherwise. We impose the Kutta condition to regularize the potential flow at the tips of the plate. In the ζ-plane the flow is non-singular since the singularity has been absorbed by the mapping. To remove the singularity in the z-plane the complex velocity (4) in the mapped plane has to be zero at the top and bottom of the circle, i.e., at $\zeta = \pm i$. Solving for Γ_1 we obtain:

$$\Gamma_1 = -\pi i \frac{(1+\zeta_1^2)(1+\bar{\zeta}_1^2)}{(\zeta_1-\bar{\zeta}_1)(1-\zeta_1\bar{\zeta}_1)}\left[2U - \sum_{n=2}^{N}\frac{i\Gamma_n}{\pi}\frac{(\zeta_n-\bar{\zeta}_n)(1-\zeta_n\bar{\zeta}_n)}{(1+\zeta_n^2)(1+\bar{\zeta}_n^2)} + s\right]. \tag{5}$$

Note that the circulation associated with the vortex pair depends on all the flow quantities, i.e., free-stream velocity U, suction s, position and circulation of all the vortex pairs, and the position of the vortex pair 1. The above expression suggests that the Kutta condition can be satisfied even when there are no vortices in the flow. It suffices to choose $s(t) = -2U(t)$ (see Figure 2).

To describe the motion of the vortex pair in the physical plane we use the following set of ordinary differential equations:

$$\begin{cases} \dfrac{d\bar{z}_1}{dt} + (\bar{z}_1 + 2i)\dfrac{1}{\Gamma_1}\dfrac{d\Gamma_1}{dt} = \lim\limits_{z\to z_1}\left\{\dfrac{d}{dz}\left[F - \dfrac{i\Gamma_1}{2\pi}\log(z-z_1)\right]\right\} \\ \dfrac{d\bar{z}_r}{dt} = \lim\limits_{z\to z_r}\left\{\dfrac{d}{dz}\left[F - \dfrac{i\Gamma_r}{2\pi}\log(z-z_r)\right]\right\}, \end{cases} \tag{6}$$

with the initial conditions:

$$\begin{cases} z_1(t_s) = 2i \\ z_r(t_s) = z_{r_s} \qquad r = 2...N. \end{cases} \tag{7}$$

The term containing $d\Gamma_1/dt$ is known as Brown and Michael's correction (Brown and Michael 1954). The motion of the vortex of variable strength described by this equation guarantees no net force on the vortex and its connecting cut. The limit on the right hand side, which represents the complex velocity at the vortex location without the self-induced contribution, produces the so called "Routh's correction" when it is evaluated in the mapped plane (e.g. Clements 1973).

We solve the problem in the mapped plane. Once we have performed the change of variables, substituted for the complex potential, and carried out the limit required in equation (6), we obtain:

$$
\begin{cases}
\left[\dfrac{\bar{\zeta}_1^2+1}{\bar{\zeta}_1^2}+\dfrac{(\bar{\zeta}_1+i)^2}{\bar{\zeta}_1}\dfrac{(1+\zeta_1^2)(1-\bar{\zeta}_1^2)}{(1+\bar{\zeta}_1^2)(\zeta_1-\bar{\zeta}_1)(1-\zeta_1\bar{\zeta}_1)}\right]\dfrac{d\bar{\zeta}_1}{dt} \\
\qquad -\left[\dfrac{(\zeta_1+i)^2}{\bar{\zeta}_1}\dfrac{(1-\zeta_1^2)(1+\bar{\zeta}_1^2)}{(1+\zeta_1^2)(\zeta_1-\bar{\zeta}_1)(1-\zeta_1\bar{\zeta}_1)}\right]\dfrac{d\zeta_1}{dt}= \\
\left(\dfrac{\zeta_1^2}{1+\zeta_1^2}\right)\left\{U\left(1-\dfrac{1}{\zeta_1^2}\right)+\dfrac{i\Gamma_1}{2\pi}\left[\dfrac{\bar{\zeta}_1}{1-\zeta_1\bar{\zeta}_1}-\dfrac{1}{\zeta_1-\bar{\zeta}_1}-\dfrac{\zeta_1}{1-\zeta_1^2}\right]+\dfrac{i\Gamma_1}{2\pi}\dfrac{1}{\zeta_1(1+\zeta_1^2)}\right. \\
\qquad \left.+\sum_{n=2}^{N}\dfrac{i\Gamma_n}{2\pi}\dfrac{(1-\zeta_1^2)(\zeta_n-\bar{\zeta}_n)(1-\zeta_n\bar{\zeta}_n)}{(\zeta_1-\zeta_n)(\zeta_1-\bar{\zeta}_n)(1-\zeta_1\zeta_n)(1-\zeta_1\bar{\zeta}_n)}-s\dfrac{\zeta_1+1}{\zeta_1(\zeta_1-1)}\right\} \\
\qquad -\dfrac{(\bar{\zeta}_1+i)^2}{\bar{\zeta}_1}\left[2\dfrac{dU}{dt}-\sum_{n=2}^{N}\dfrac{i\Gamma_n}{\pi}\left[\dfrac{1-\zeta_n^2}{(1+\zeta_n^2)^2}\dfrac{d\zeta_n}{dt}-\dfrac{1-\bar{\zeta}_n^2}{(1+\bar{\zeta}_n^2)^2}\dfrac{d\bar{\zeta}_n}{dt}\right]+\dfrac{ds}{dt}\right] \\
\qquad \times\left[2U-\sum_{n=2}^{N}\dfrac{i\Gamma_n}{\pi}\dfrac{(\zeta_n-\bar{\zeta}_n)(1-\zeta_n\bar{\zeta}_n)}{(1+\zeta_n^2)(1+\bar{\zeta}_n^2)}+s\right]^{-1} \\
\dfrac{d\bar{\zeta}_r}{dt}=\left[\dfrac{\zeta_r^2\bar{\zeta}_r^2}{(1+\zeta_r^2)(1+\bar{\zeta}_r^2)}\right]\left\{U\left(1-\dfrac{1}{\zeta_r^2}\right)+\dfrac{i\Gamma_r}{2\pi}\left[\dfrac{\bar{\zeta}_r}{1-\zeta_r\bar{\zeta}_r}-\dfrac{1}{\zeta_r-\bar{\zeta}_r}-\dfrac{\zeta_r}{1-\zeta_r^2}\right]\right. \\
\qquad \left.+\dfrac{i\Gamma_r}{2\pi}\dfrac{1}{\zeta_r(1+\zeta_r^2)}+\sum_{n\neq r}^{N}\dfrac{i\Gamma_n}{2\pi}\dfrac{(1-\zeta_r^2)(\zeta_n-\bar{\zeta}_n)(1-\zeta_n\bar{\zeta}_n)}{(\zeta_r-\zeta_n)(\zeta_r-\bar{\zeta}_n)(1-\zeta_r\zeta_n)(1-\zeta_r\bar{\zeta}_n)}-s\dfrac{\zeta_r+1}{\zeta_r(\zeta_r-1)}\right\},
\end{cases}
\tag{8}
$$

with the initial conditions:

$$
\begin{cases}
\zeta_1(t_s)=i \\
\zeta_r(t_s)=\zeta_{r_s} \qquad r=2...N,
\end{cases}
\tag{9}
$$

where Γ_1 is given by (5). Note that because of Brown and Michael's correction the equations are coupled not only through the position of the vortices but also through the velocity of the vortices.

The forces acting on the plate are of particular interest because they can be measured experimentally and are the crucial quantities in any problem involving the interaction between fluids and structures. The forces can be computed by means of the Blasius theorem, see Cheers 1979, Graham 1980, and Cortelezzi 1995 for different derivations. The drag has the following form:

$$
D=4\pi\rho\frac{dU}{dt}+4\pi\rho\frac{ds}{dt}+i\rho\frac{d}{dt}\left[\frac{\Gamma_1(1-\zeta_1\bar{\zeta}_1)(\zeta_1-\bar{\zeta}_1)}{\zeta_1\bar{\zeta}_1}\right]+i\rho\sum_{n=2}^{N}\Gamma_n\frac{d}{dt}\left[\frac{(1-\zeta_n\bar{\zeta}_n)(\zeta_n-\bar{\zeta}_n)}{\zeta_n\bar{\zeta}_n}\right]. \tag{10}
$$

The component of the force along the imaginary axis, which represents the lift, is zero because of the imposed symmetry. The first term on the right hand side is the force due to added mass, i.e., the inertia of the attached flow, while the second term is the contribution due to suction, and the last two terms are the contributions due to the evolution of the wake. We define the drag coefficient as follows:

$$
C_D=\frac{D}{\frac{1}{2}\rho U_\infty^2 L} \tag{11}
$$

Note that the drag coefficient is well defined only in the case where the free-stream velocity is constant. In order to compute the drag coefficient in the unsteady cases that we present in Section 5, we choose for U_∞ the asymptotic value or the mean value of the free-stream velocity.

The final element necessary for a correct implementation of this model is a vortex shedding mechanism. If we envision the separation process by means of a vortex sheet, then the instantaneous circulation necessary to keep the flow regular at the tip of the plate is associated with an infinitesimal segment of the sheet which is shed in the fluid. Consequently, the circulation is distributed along the singular line and the sheet rolls-up around the points of greatest absolute circulation per unit length, and it stretches most where the absolute circulation per unit length is smallest. As the process continues, we observe that a large amount of circulation concentrates in the core of the spirals which are connected to each other by filaments of almost negligible circulation. This process can be reflected in our model by replacing each spiral with a point vortex of fixed circulation, except for the spiral connected to the separation point which is replaced by a point vortex with time-dependent circulation. This latter vortex will continue to be fed circulation until the rate of change of circulation becomes zero because we conjecture that this is the part of the sheet that will be stretched the most.

Let us consider the problem of shedding a new vortex when $N-1$ other vortices are already present in the flow. If t_s is the shedding time, then it is crucial to analyze the transition from t_s^- to t_s^+. Up to the time t_s^-, the variable strength of vortex 1 satisfies the Kutta condition. At time $t = t_s$, the strength of this vortex is frozen and all the vortices are renumbered. Finally at t_s^+ a new vortex 1 is introduced into the flow to remove the square root singularity. If we restrict our simulation to the case where the shed vortices have alternate sign, then we can model the vortex shedding by making the assumption that the time $t = t_s$ is determined by the condition:

$$\left.\frac{d\Gamma_1}{dt}\right|_{t=t_s} = 0, \tag{12}$$

assuming $d^2\Gamma_1/dt^2\big|_{t=t_s} \neq 0$. Any other choice for the shedding time implies the arbitrary production of two sequential vortices of the same sign or the existence of a vortex whose strength decreases in time. The latter situation is physically unacceptable. This procedure has been proposed by Graham (1980) to simulate the flow induced by an oscillating diamond shaped cylinder.

The quality of the simulation with many vortices depends in large part on the shedding mechanism. Let us assume that between two zero crossings $d\Gamma_1/dt$ is positive and has two peaks, then it is not clear whether one or two vortices should be shed during this period. It seems that the deepness of the trough separating the peaks would be an important parameter. If it is very deep it seems reasonable to have two vortices, otherwise one is sufficient. Although the shedding mechanism can be implemented for all cases, to avoid any ambiguity we restrict ourselves to cases where the rate of circulation production has only one local maximum or minimum between consecutive zero crossings or, equivalently, where $d^2\Gamma_1/dt^2$ does not change sign between crossings.

Because of the size and complexity of the problem we are not attempting to obtain an analytical solution. We solve the problem numerically using the methods described in our previous work (Cortelezzi 1995).

3 Active wake control

There are different approaches one can use to control the wake past a plate by suction. One can try to control the position of the vortices or some features of the velocity field. We choose to control the amount of circulation injected in the flow because we believe that this is the most efficient way to control the wake. To gain insight on the effectiveness of the suction as a mean to control the circulation, we compute the rate of circulation production by taking the time derivative of (5)

$$\begin{aligned}\frac{d\Gamma_1}{dt} = &-\frac{\pi i}{(\zeta_1-\bar{\zeta}_1)(1-\zeta_1\bar{\zeta}_1)}\left[2U-\sum_{n=2}^{N}\frac{i\Gamma_n}{\pi}\frac{(\zeta_n-\bar{\zeta}_n)(1-\zeta_n\bar{\zeta}_n)}{(1+\zeta_n^2)(1+\bar{\zeta}_n^2)}+s\right]\\ &\times\left[(1+\bar{\zeta}_1^2)^2(1-\zeta_1^2)\frac{d\zeta_1}{dt}-(1+\zeta_1^2)^2(1-\bar{\zeta}_1^2)\frac{d\bar{\zeta}_1}{dt}\right]\\ &-\pi i\frac{(1+\zeta_1^2)(1+\bar{\zeta}_1^2)}{(\zeta_1-\bar{\zeta}_1)(1-\zeta_1\bar{\zeta}_1)}\left[2\frac{dU}{dt}-\sum_{n=2}^{N}\frac{i\Gamma_n}{\pi}\left[\frac{1-\zeta_n^2}{(1+\zeta_n^2)^2}\frac{d\zeta_n}{dt}-\frac{1-\bar{\zeta}_n^2}{(1+\bar{\zeta}_n^2)^2}\frac{d\bar{\zeta}_n}{dt}\right]+\frac{ds}{dt}\right].\end{aligned} \tag{13}$$

From the above expression we see that the rate of circulation production depends on all flow quantities and their derivatives. Note that suction and rate of change of suction contribute to the production of circulation in the same way as free-stream velocity and free-stream acceleration, respectively. Hence, using suction as a means to control the rate of circulation production is as powerful as using the free-stream velocity.

Our control objective is to inhibit the rate of circulation production after the starting vortex pair is shed in the flow. In other words, we want to predict the suction so that once the starting vortex pair is shed in the flow the Kutta condition remains satisfied without requiring a new vortex pair. The possibility to maintain the wake confined to a controlled recirculating bubble has important implication to the problem of drag reduction in general. Moreover it can provide insight into vortex management techniques for the three-dimensional flow over a delta wing (see Rao 1987). Note that there is no conceptual difficulty in inhibiting the rate of circulation production when more than one vortex pair in present in the wake, if it is required by the application under consideration.

Let t_s be the time when the starting vortex pair is shed in the flow, i.e. the time when the rate of circulation production is zero. Then for $0 \le t \le t_s$ the motion of the vortex pair of time-dependent circulation is prescribed by the following equation:

$$\begin{aligned}&\left[\frac{\bar{\zeta}_1^2+1}{\bar{\zeta}_1^2}+\frac{(\bar{\zeta}_1+i)^2}{\bar{\zeta}_1}\frac{(1+\zeta_1^2)(1-\bar{\zeta}_1^2)}{(1+\bar{\zeta}_1^2)(\zeta_1-\bar{\zeta}_1)(1-\zeta_1\bar{\zeta}_1)}\right]\frac{d\bar{\zeta}_1}{dt}\\ &\qquad-\left[\frac{(\bar{\zeta}_1+i)^2}{\bar{\zeta}_1}\frac{(1-\zeta_1^2)(1+\bar{\zeta}_1^2)}{(1+\zeta_1^2)(\zeta_1-\bar{\zeta}_1)(1-\zeta_1\bar{\zeta}_1)}\right]\frac{d\zeta_1}{dt}=\\ &\left(\frac{\zeta_1^2}{1+\zeta_1^2}\right)\left\{U\left(1-\frac{1}{\zeta_1^2}\right)+\frac{i\Gamma_1}{2\pi}\left[\frac{\bar{\zeta}_1}{1-\zeta_1\bar{\zeta}_1}-\frac{1}{\zeta_1-\bar{\zeta}_1}-\frac{\zeta_1}{1-\zeta_1^2}\right]\right.\\ &\qquad\left.+\frac{i\Gamma_1}{2\pi}\frac{1}{\zeta_1(1+\zeta_1^2)}-s\frac{\zeta_1+1}{\zeta_1(\zeta_1-1)}\right\}-\frac{(\bar{\zeta}_1+i)^2}{\bar{\zeta}_1}\left[2\frac{dU}{dt}+\frac{ds}{dt}\right][2U+s]^{-1}\end{aligned} \tag{14}$$

with the initial condition:

$$\zeta_1(0) = i. \tag{15}$$

Note that suction appears in the above equation but in this study it is not used to control the flow for $t \leq t_s$. In general, suction can be used to drive the system to some desired state at $t = t_s$, from which the controller that inhibits the production of circulation takes over.

When $t \geq t_s$ the equation of motion for the vortex pair of constant circulation $\pm\Gamma_{1_s}$ is:

$$\frac{d\bar{\zeta}_1}{dt} = \left[\frac{\zeta_1^2\bar{\zeta}_1^2}{(1+\zeta_1^2)(1+\bar{\zeta}_1^2)}\right]\left\{U\left(1-\frac{1}{\zeta_1^2}\right)+\frac{i\Gamma_{1_s}}{2\pi}\left[\frac{\bar{\zeta}_1}{1-\zeta_1\bar{\zeta}_1}-\frac{1}{\zeta_1-\bar{\zeta}_1}-\frac{\zeta_1}{1-\zeta_1^2}\right]\right.$$
$$\left.+\frac{i\Gamma_{1_s}}{2\pi}\frac{1}{\zeta_1(1+\zeta_1^2)}-s\frac{\zeta_1+1}{\zeta_1(\zeta_1-1)}\right\}, \tag{16}$$

with the initial condition:

$$\zeta_1(t_s) = \zeta_{1_s}. \tag{17}$$

To close the problem we have to provide an equation for s which implements our control strategy. An ordinary differential equation for s can be obtained from (13) simply by setting $d\Gamma_1/dt = 0$, and $\Gamma_n = 0$, for $n = 2, 3, ..., N$. Nevertheless, a simpler result follows from the fact that the problem of maintaining $d\Gamma_1/dt = 0$, $\forall t > t_s$, is equivalent to the problem of maintaining the Kutta condition satisfied when a vortex pair of fixed circulation is present in the flow. Then the suction which implements our control strategy is simply derived by solving (5) for s when $\Gamma_n = 0$, $n = 2, 3, ..., N$. We have:

$$s = -2U - \pi i\Gamma_{1_s}\frac{(\zeta_1-\bar{\zeta}_1)(1-\zeta_1\bar{\zeta}_1)}{(1+\zeta_1^2)(1+\bar{\zeta}_1^2)}. \tag{18}$$

A question arises about the compatibility of the equations (14) and (16). Compatibility is required to guarantee a smooth transition, at time $t = t_s$, from the final state of equation (14) to the initial state of equation (16). At time $t = t_s$ the Brown and Michael correction vanishes and the two equation coincide, consequently insuring compatibility.

4 Dynamical behavior of the controlled system

In the previous section we have been able to find a controller which inhibits the production of circulation when a vortex pair is present in the flow. This section is devoted to the analysis of the dynamical behavior of the controlled system.

As an initial step we solve for the fixed points of the unperturbed system. For convenience we rewrite equation (16) in polar form (see Figure 1). We obtain:

$$\begin{cases} \dfrac{d\rho_1}{dt} = \dfrac{\rho_1}{\rho_1^4+1-2\rho_1^2\cos 2\theta_1}\left[U\rho_1(\rho_1^2-1)\sin\theta_1 - \dfrac{s\rho_1^2(\rho_1^2-1)}{\rho_1+1-2\rho_1\sin\theta_1}\right. \\ \qquad\qquad \left. + \dfrac{\Gamma_{1_s}\rho_1^2[8\rho_1^2(\rho_1^4+1-2\rho_1^2\sin\theta_1)\cos^2\theta_1-(\rho_1^4-1)^2]\sin\theta_1}{4\pi[(\rho_1^4+1)^2-4\rho_1^2\cos^2 2\theta_1]\cos\theta_1}\right] \\ \dfrac{d\theta_1}{dt} = \dfrac{\rho_1}{\rho_1^4+1-2\rho_1^2\cos 2\theta_1}\left[U(\rho_1^2+1)\cos\theta_1 + \dfrac{2s\rho_1^2\cos\theta_1}{\rho_1+1-2\rho_1\sin\theta_1}\right. \\ \qquad\qquad \left. + \dfrac{\Gamma_{1_s}\rho_1(\rho_1^2+1)[8\rho_1^2(\rho_1^4+1-2\rho_1^2\cos\theta_1)\cos^2\theta_1+(\rho_1^2-1)^4]}{4\pi(\rho_1^2-1)[(\rho_1^4+1)^2-4\rho_1^2\cos^2 2\theta_1]}\right] \end{cases} \tag{19}$$

where

$$s = \frac{\Gamma_{1_s}}{\pi} \frac{2\rho_1(\rho_1^2 - 1)\cos\theta_1}{\rho_1^4 + 1 - 2\rho_1^2\cos 2\theta_1} - 2U. \tag{20}$$

Note that in the above equations the free-stream velocity is indicated with U for clarity although it is simply unity. Consequently, the problem depend only on one parameter, namely the circulation Γ_{1_s} of the vortex.

When suction is zero there does not exist any vortex pair which is stationary and satisfies the Kutta condition, aside from the pathological situation where the vortex pair has infinite circulation and is infinitely distant from the plate. This result predicts that, for any free-stream velocity, a flow which separates from the tips of a flat plate cannot reach a steady-state solution. To the best of our knowledge there is no experimental evidence which contradicts this prediction. When suction is non-zero, there are fixed points and their locus is shown in Figure 4. Each point on this curve represents the position of a vortex which is stationary and satisfies the Kutta condition, and whose circulation is shown in Figure 5(b). The suction associated with each fixed point is shown in Figure 5(a). The reader should be aware that we restrict our discussion to the upper half of the domain due to the symmetry of the problem.

We derive a linear stability analysis to investigate the nature of the fixed points. Figure 3 shows the real and imaginary parts of the eigenvalues λ_1 and λ_2. Three distinct regions can be recognized. Near the plate, where $0 < x < x_1$, the eigenvalues λ_1 and λ_2 are complex conjugates with positive real parts (see Figure 3). In this region the fixed points are unstable foci. Figure 5 shows that both, circulation and suction, are negative. Physically it means that the Kutta condition is unusually satisfied by a vortex generating a counterclockwise flow and by injecting fluid. In particular, when $x = 0$, there are no vortices in the flow and the case shown in Figure 2 is recovered. In the middle region, where $x_1 < x < x_2$, the eigenvalues are purely real with $\lambda_1 < \lambda_2 < 0$ (see Figure 3). In this region the fixed points are stable nodes. Circulation and suction are both positive as expected (see Figure 5). Note that the values of circulation and of suction at $x = x_2^-$ are the minimum values necessary to have a stable fixed point, that is $\Gamma_c \approx 18.49$ and $s_c \approx 0.67$ respectively. Note also that the asymptote at $x = x_1$ separates two regions with totally different dynamics. No smooth transition is possible between the two regions since both circulation and suction are discontinuous at $x = x_1$. In the third region, where $x > x_2$, the eigenvalues are purely real with $\lambda_1 < 0 < \lambda_2$ (see Figure 3). In this region the fixed points are saddle points. As before, circulation and suction are both positive, see (Figure 5). The circulation increases from Γ_c to infinity while the suction decreases monotonically to zero as x goes from x_2 to infinity. Note that at $x = x_2$ the eigenvalue λ_2 is zero, this fact represents a sufficient condition for the bifurcation of a fixed point.

We restrict our discussion to the sub-domain where $x > x_1$, $\Gamma_{1_s} > 0$, and $s > 0$. It is important to observe that in this sub-domain there are fixed points only when $\Gamma_{1_s} \geq \Gamma_c$. As suggested by the behavior of the eigenvalue λ_2, the vector field undergoes a saddle-node bifurcation at $x = x_2$ when $\Gamma_{1_s} = \Gamma_c$. Hence, the circulation Γ_{1_s} plays the role of bifurcation parameter. Technically, the bifurcation should be analyzed using the center manifold theorem (see Guckenheimer and Holmes, Chp.4), but to maintain the paper focused on fluid-mechanics we skip this formal step. To document the effect of the bifurcation parameter and to give a complete characterization of the dynamics of

the system, we plot the sub-space of the phase space which coincides with the physical domain. In this plane the lines of flow of the vector field coincide with the trajectories of the vortex. The reader should be aware that these trajectories are obtained for constant free-stream velocity and circulation while suction in general changes along each trajectory. When $\Gamma_{1_s} < \Gamma_c$ there are no fixed points. There are only two families of trajectories delimited by a separatrix (see Figure 6(a)). When a vortex starts above the separatrix it drifts irreversibly downstream. When, instead, the vortex starts below the separatrix, depending on its initial position, it can approach temporarily the plate, but eventually it drifts downstream. When $\Gamma_{1_s} = \Gamma_c$ there is a non-hyperbolic fixed point and the flow pattern of the center manifold can be easily recognized (see Figure 6(b)). Finally, when $\Gamma_{1_s} > \Gamma_c$ there are two hyperbolic fixed points: a stable node and a saddle point (see Figure 6(c)). The vortex trajectory is characterized by the initial position of the vortex with respect to the stable manifold of the saddle point. If the vortex is initially on the left of the stable manifold, then it is driven by the controller to the stable node. It is interesting to observe that the trajectories between the stable manifold and the x-axis extend infinitely downstream. When the vortex and its image are initially in the narrow region delimited by the stable manifold and the image manifold, they propel themselves upstream, and with the help of suction they first approach the plate and then are driven to the stable node and its image. When, instead, the vortex is initially on the right of the stable manifold it drifts downstream even if it temporarily approaches the plate. We define the controllability region as the basin of attraction of the stable node, i.e., the region delimited by the coordinate axes and the stable manifold of the saddle point. Note that as Γ_{1_s} increases, the distance between stable node and saddle point also increases, with a consequent widening of the controllability region.

Since our final goal is to control the wake past the plate in the presence of an unsteady free-stream condition, it is crucial to investigate how the phase space changes under a time-dependent perturbation. The answer to this question is given by a theorem (see Guckenheimer and Holmes, Chp. 4) which guarantees that the Poincaré section of a periodically perturbed system is topologically equivalent, for sufficiently small perturbations, to the phase space of the unperturbed system provided that the fixed points are hyperbolic. We perturb our system with a free-stream velocity of the form $U(t) = 1 + \epsilon \sin(\omega t)$ and compute the Poincaré section by plotting the vortex position at $t = 2n\pi/\omega$ for $n = 0, 1, 2, \ldots$. The resulting Poincaré section presents two hyperbolic fixed points: a stable node and a saddle point, see Figure 6(d). The stable node represents a limit cycle and the saddle point an unstable periodic orbit. As we show in the next section (see Figure 13), the vortex is driven to a periodic orbit if it is initially on the left of the stable manifold of the Poincaré section. The topological equivalence between the phase space and the Poincaré section becomes evident by comparing Figures 6(c) and 6(d). Because of this equivalence we can extend the definition of controllability region to the perturbed system. The controllability region coincides with the basin of attraction of the stable node of the Poincaré section.

In conclusion, suction is a powerful mean to control the wake past a plate both in perturbed and unperturbed conditions provided that the vortex is initially within the controllability region. In the unperturbed case the vortex is driven to the stable node while in the periodically perturbed case is driven to a periodic orbit.

5 Results

In this section we present the results of three simulations. The first two simulations document the ability of the controller to drive the vortex to the stable node when the free-stream velocity is constant, or to a limit cycle when the free-stream velocity oscillates periodically. The third simulation documents the performance of the controller when the free-stream velocity oscillates pseudo-randomly.

In the first simulation the free-stream velocity increases from rest, reaches a maximum value, and decreases to a unit value at $t = 1$ (see Figure 7). We carefully choose the initial evolution of the free-stream velocity so that, in all three simulations, a vortex pair of nearly the same circulation $\Gamma_{1_s} > \Gamma_c$ is shed in the flow at nearly the same time. For simplicity suction is used to control the wake only after the rate of circulation production has gone to zero (see Figures 7 and 9). Three distinct time intervals can be recognized. Initially, when $0 < t < t_s$, the flow is uncontrolled and separates from the tips of the plate creating a vortex pair which drifts downstream. Figure 8 shows the trajectory of the top vortex. The rate of circulation production associated with the top vortex increases initially, decreases during the deceleration, and eventually become zero at $t = t_s \approx 0.71$ thereby triggering the controller (see Figure 9). At the same time the circulation of the top vortex reaches its maximum and final value (see Figure 9). The drag is dominated by the effect of the added mass because of the strong accelerations of the flow (see Figure 10). In the second interval, $t_s < t < 1$, the controller predicts the suction necessary to maintain the wake to a single vortex pair of constant circulation, $\Gamma_{1_s} = \pm 20.01$ (see Figures 7 and 9). The flow is still decelerating and the suction increases rapidly driving the vortices away from their drifting trajectories and toward the x-axis (see Figures 7 and 8). The drag increases suddenly because of the effect of suction, but quickly decreases and becomes negative as the effect of the added mass returns to dominate (see Figure 10). Finally, when $t > 1$, free-stream velocity and circulation are constants and suction drives the vortex pair to the stable node. Note that the vortex pair moves on the trajectory predicted by the analysis in Section 4 (see for a comparison Figures 6(c) and 8). The drag increases from its minimum value and eventually reaches a zero value as the added mass effect subdues (see Figure 10). Figures 11(a)-(f) show the instantaneous streamlines during the capturing process; because of symmetry we plot only the top half of the domain. Figure 11(a) and (b) show the flow at time $t < t_s$, where two recirculating bubbles grow and merge together. As suction becomes non-zero the recirculating bubble splits again into two bubbles (see Figure 11(c)). Figures 11(c)-(f) show how the vortex is driven to the fixed point. Figures 11(e)-(f) are nearly identical because the flow has almost reached its steady state.

In the second simulation the free-stream velocity increases from rest and reaches a maximum value, as in the first simulation, but then oscillates about unit mean value (see Figure 12). Note that the amplitude of the oscillations is such that the flow reverses its direction for nearly one third of the period of oscillation, creating one of the worst possible scenario for the controller. Three distinct intervals of time can be recognized. Initially, when $0 < t < t_s$, the flow behaves qualitatively

as in the first simulation (see Figures 12-15). The rate of circulation production becomes zero at $t = t_s \approx 0.69$. In the second interval, $t_s < t < 2$, the controller predicts the suction necessary to maintain the wake to a single vortex pair of constant circulation, $\Gamma_{1_s} \approx \pm 20.04$ (see Figures 12 and 14). Suction increases at first, then after a fluctuation it reaches its maximum absolute value, and finally suction decreases sharply. As a result the vortices are driven away from their drifting trajectories, at first toward the origin and then toward the tip of the plate. At the end of the first period the vortices are positioned near the limit cycle trajectories (see Figure 13). The drag increases suddenly because of the effect of suction, then decreases because of the added mass effect, and finally presents a sharp peak because of the combined effects of flow acceleration and suction fluctuation (see Figure 15). Finally, when $t > 2$, all the flow quantities reach rapidly their final periodic behavior while the circulation of the vortex pair is maintained constant, see Figures 12-15. The vortices are rapidly driven to the limit cycle trajectories where they orbit during the rest of the simulation, see Figure 13. Figures 16(a)-(l) show the instantaneous streamlines during one period of oscillation, $6 < t < 8$, as the vortices move clockwise on the limit cycle trajectories.

In the final simulation the free-stream velocity increases from rest and reaches a maximum value, as in the previous simulations, but then oscillates pseudo-randomly about unit mean value (see Figure 17). Initially, when $0 < t < t_s$, the flow behaves qualitatively as in the previous simulations (see Figures 17-20). At time $t = t_s \approx 0.70$ the rate of circulation production goes to zero, triggering the controller which maintains the wake for the rest of the simulation to a single vortex pair of constant circulation, $\Gamma_{1_s} \approx \pm 20.15$ (see Figures 17 and 19). Because of the pseudo-random character of the the free-stream velocity it is difficult to give an interpretation to the time evolution of suction in term of the evolution of the flow. We can only say that suction is able to maintain the vortices orbiting on rather complex trajectories close to the plate. Note that the trajectories somehow entangles around the position of the stable nodes of the unperturbed system (see Figures 6(c) and 18).

6 Conclusions

A point vortex model has been used to simulate the unsteady separated flow past a flat plate with a suction point on the downstream wall. For this model we derived a control strategy that confines the wake to a single vortex pair of constant circulation. Due to the simplicity of the model we obtained the analytical closed-form solution of the nonlinear controller for any free-stream velocity. The performance of the controller was characterized by a dynamical system type of analysis. In the case of steady flow we computed the locus of the fixed points of the unperturbed system. We showed that a pair of stable nodes and a pair of saddle points exist only if the circulation associated with the vortex pair is above a critical value. We also showed that the vector field presents a saddle-node bifurcation and that the circulation is the bifurcation parameter. We identified the controllable region of the unperturbed system with the basins of attraction of the nodes. In the case of unsteady flow we computed the Poincaré section of the perturbed system. We presented evidence of the topological equivalence between phase space of the unperturbed system and Poincaré section. We showed that under perturbation the stable nodes of the unperturbed system become periodic

orbits. We identified the controllable region of the perturbed system as the basin of attraction of the nodes of the Poincaré section. The predictions of our analysis were verified by testing the controller with three different unsteady free-stream conditions. The first simulation documented the ability of the controller to drive the vortex pair to the stable nodes when the free-stream is asymptotically constant. The second simulation documented the ability of the controller to drive the vortex pair to the periodic orbits when the free-stream velocity oscillates periodically about a unit mean. Finally, the third simulation showed the successful performance of the controller when the free-stream velocity oscillates pseudo-randomly about a unit mean.

The present study showed that the use of a reduced model provides a favorable environment to derive the desired control strategy and to test its performance and robustness. The natural continuation of the present work would be to embed the derived controller into a more complex and realistic model, for example, the Navier-Stokes equations. The embedding process should be supported by a dynamical system and time series analysis to demonstrate the dynamical equivalence of the two models. Testing the controller in a different numerical environment instead of in an experiment presents several advantages. All the flow quantities necessary to feedback to the controller can be easily measured. The action of the controller is automatically synchronized with the evolution of the flow. Finally, the controller can be easily tested on gradually more complex flows allowing the researcher to make the controller progressively robust with respect to different types of perturbations (e.g. viscosity, three-dimensionality, back-ground noise, etc.). Successful completion of this process would open the possibilities for the active control of large-scale coherent vortical structures in engineering applications.

7 Acknowledgments

The author wishes to thank Dr. F.E. Marble for suggesting the use of a suction point as a means to control the flow. The author also wishes to thank Dr. R. Camassa and Dr. J.S. Gibson for several valuable discussions. This work was supported by the Air Force Office for Scientific Research Grant # F49620-92-J-0279.

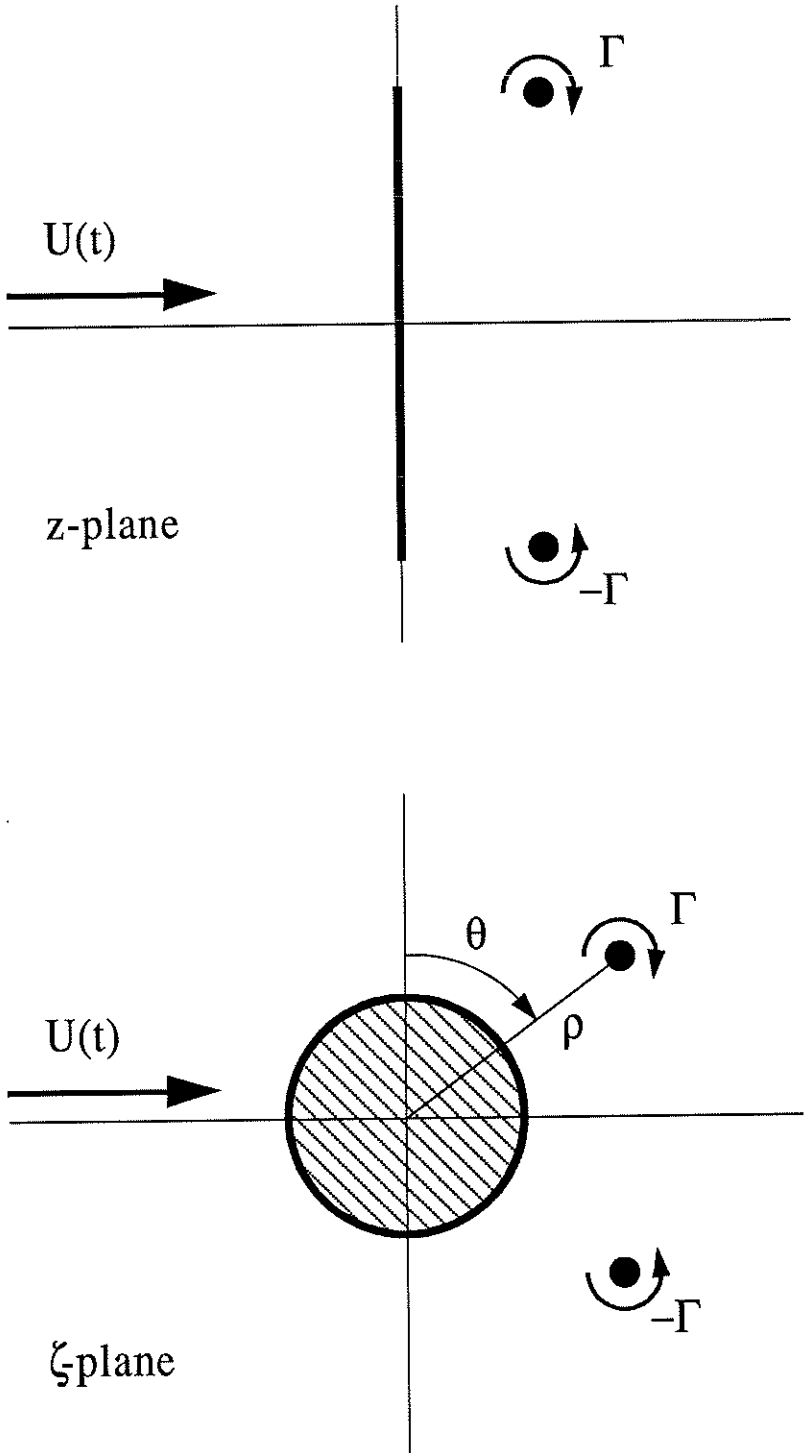

Figure 1: Physical and mapped planes for the flow past a flat plate.

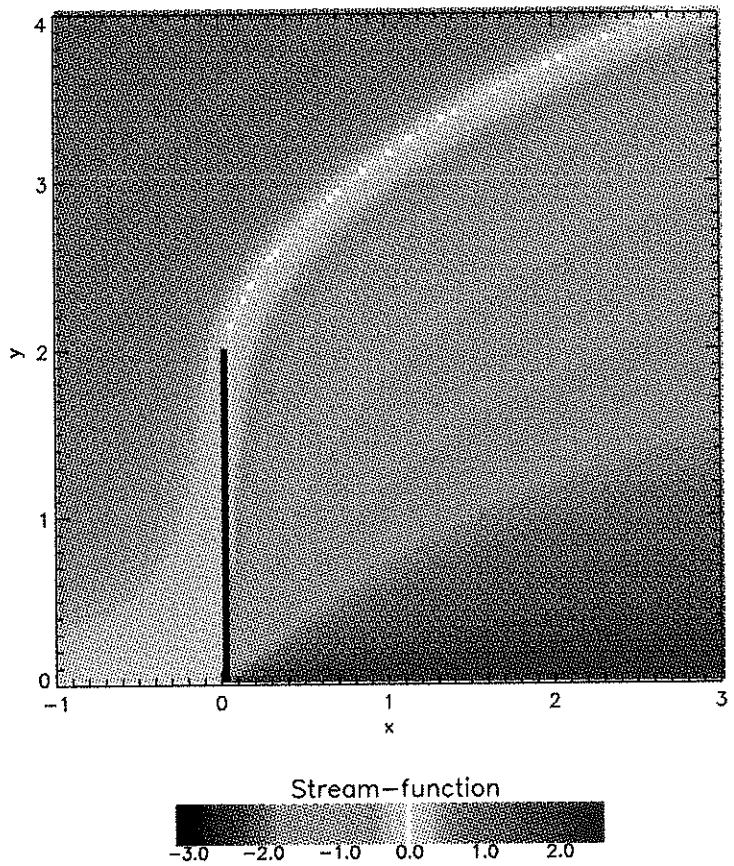

Figure 2: Instantaneous stream-function, $s = -2U$.

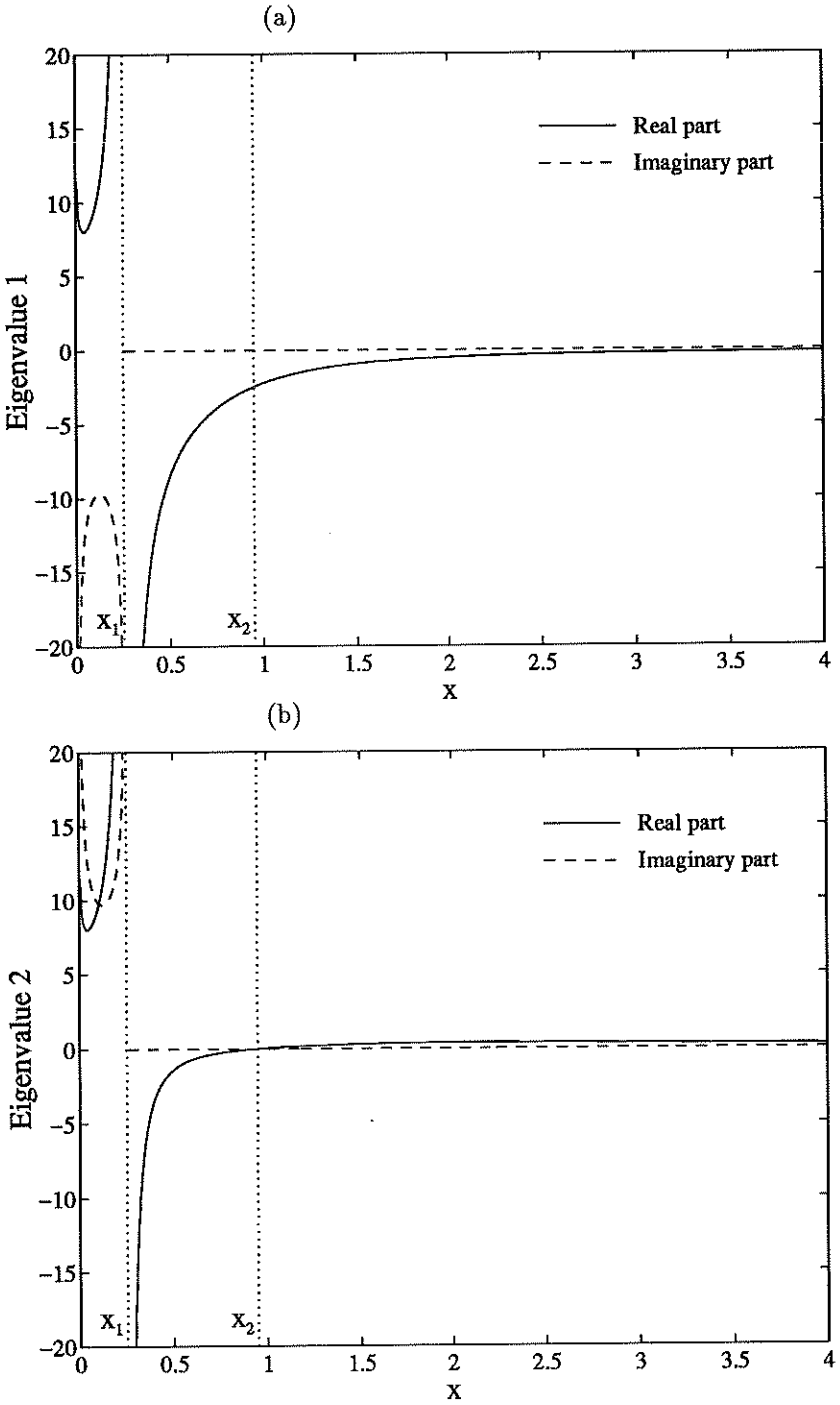

Figure 3: Real and imaginary parts of the eigenvalues λ_1 (a) and λ_2 (b).

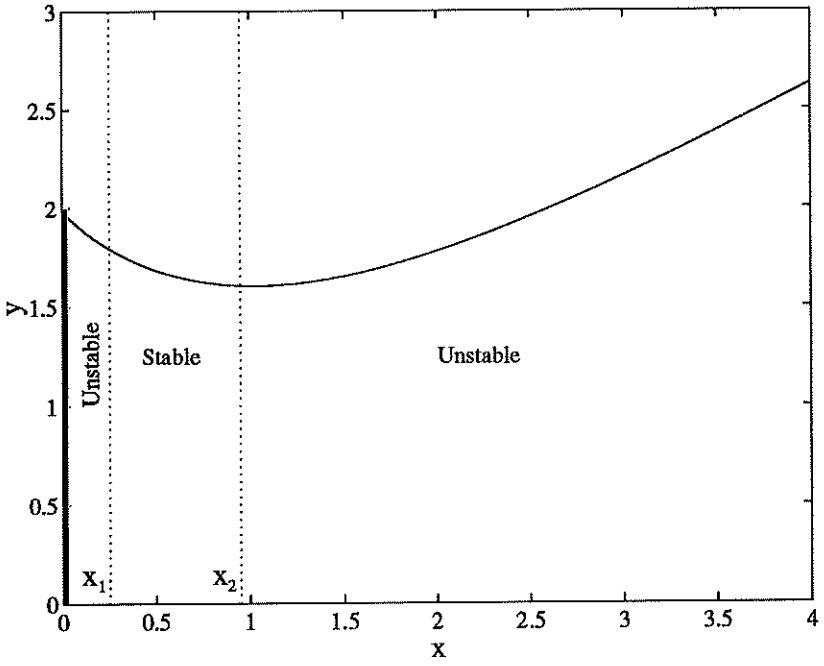

Figure 4: Locus of the fixed points.

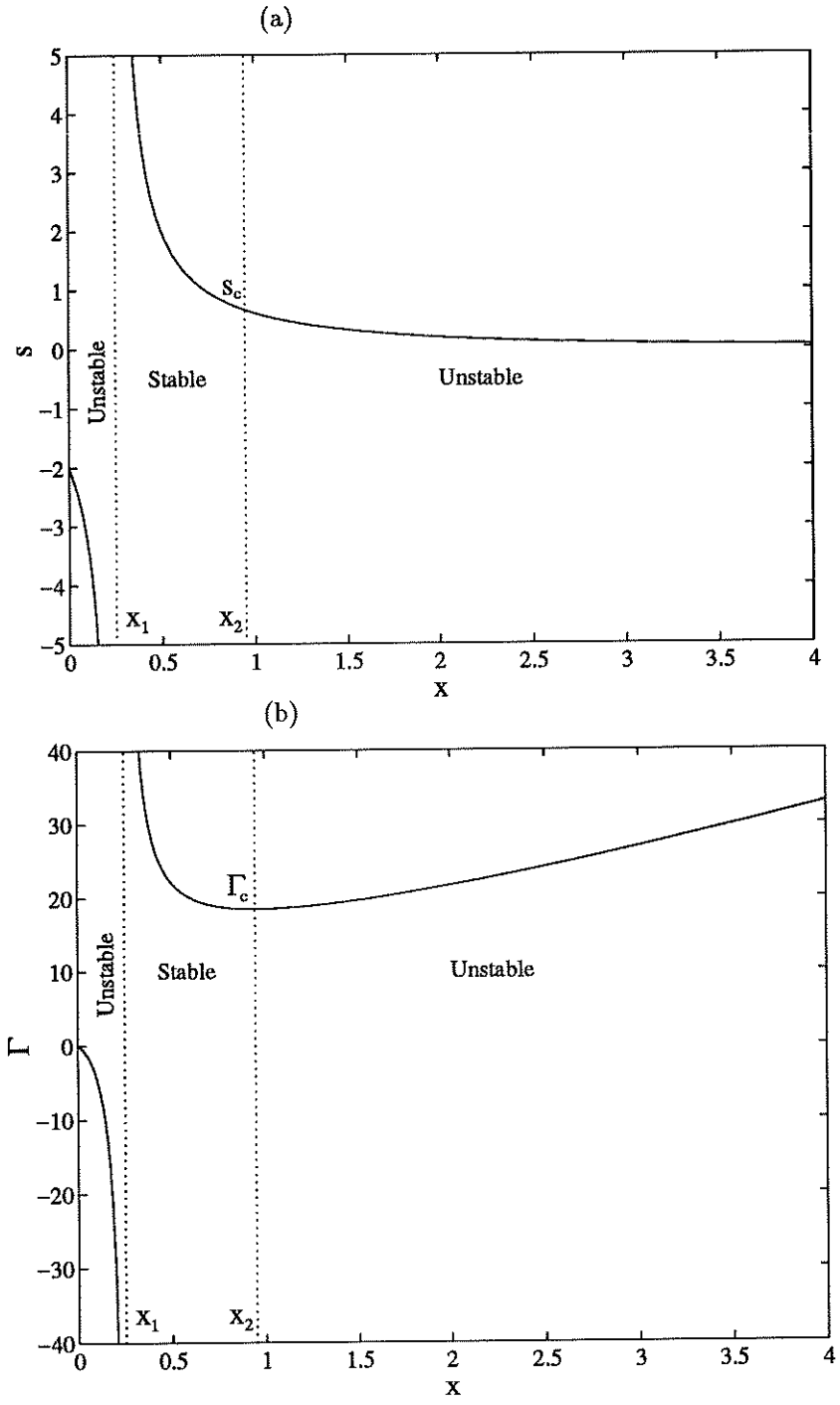

Figure 5: Suction (a) and circulation of the top vortex (b).

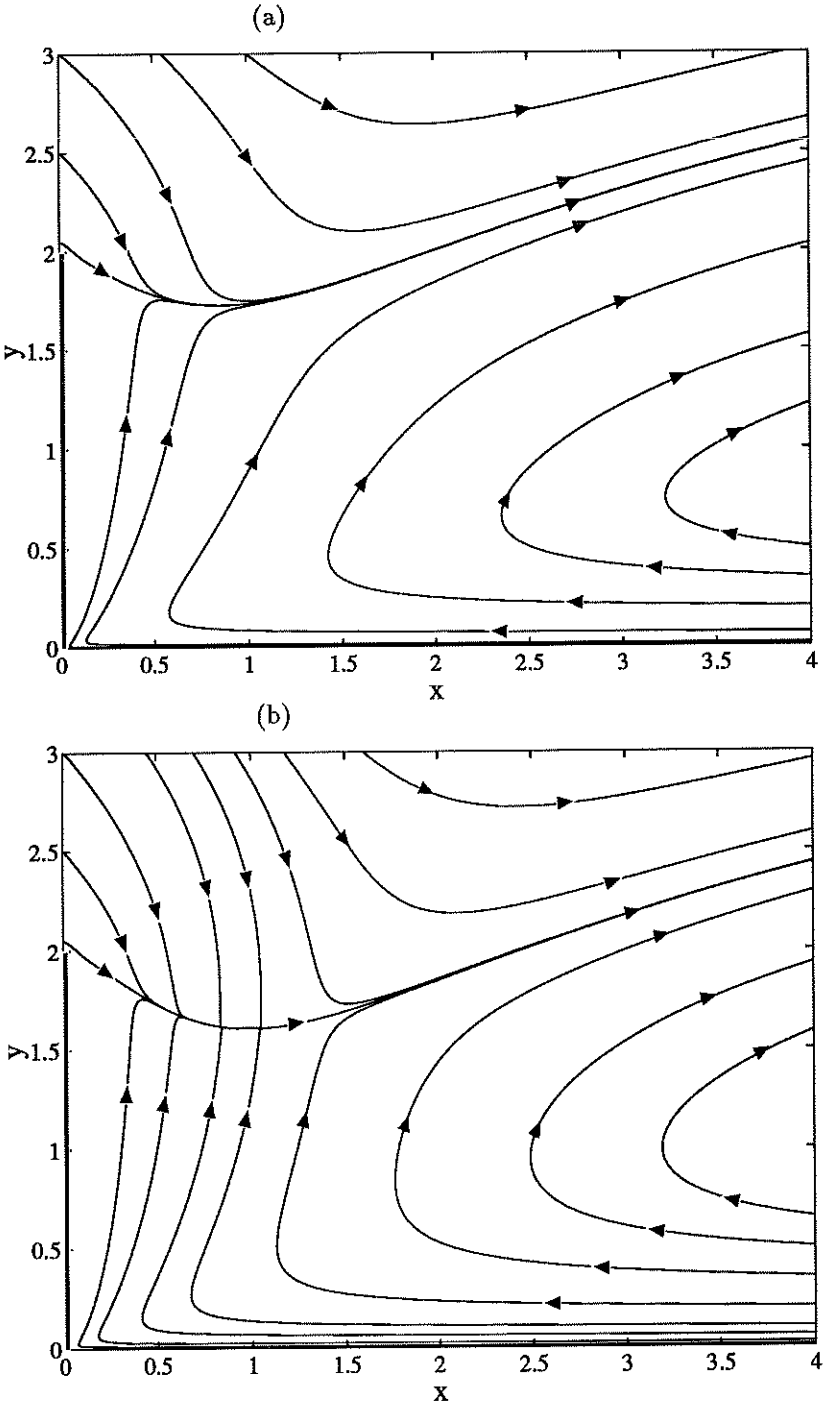

Figure 6: Vortex trajectories, $U = 1$: $\Gamma_{1_s} = 15$ (a), $\Gamma_{1_s} = 18.49(b)$.

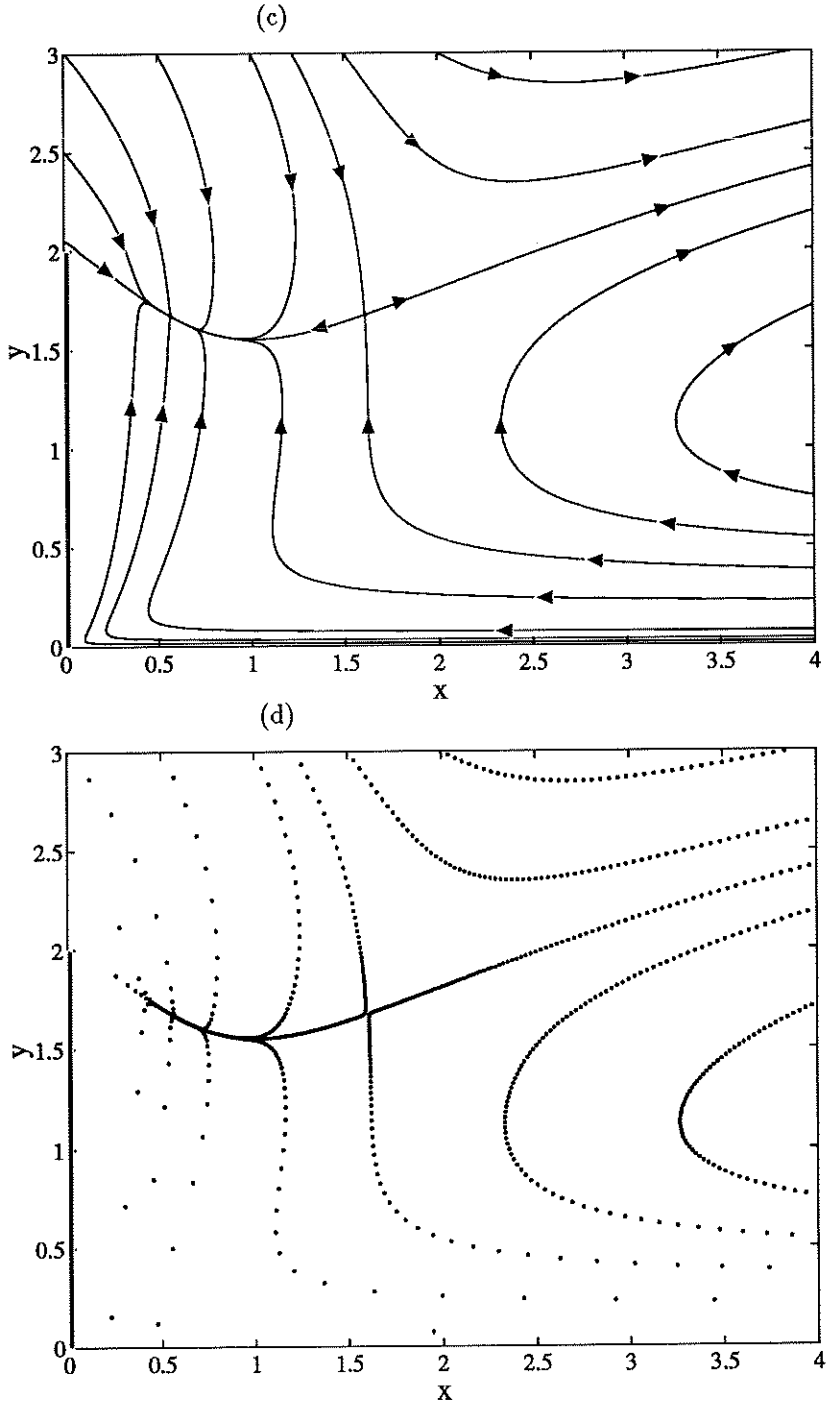

Figure 6: (Continued) Vortex trajectories, $U = 1$, $\Gamma_{1_s} = 20$ (c); Poincaré section, $U = 1 + \epsilon \sin(\omega t)$, $\epsilon = 0.1$, $\omega = 20\pi$, $\Gamma_{1_s} = 20$ (d).

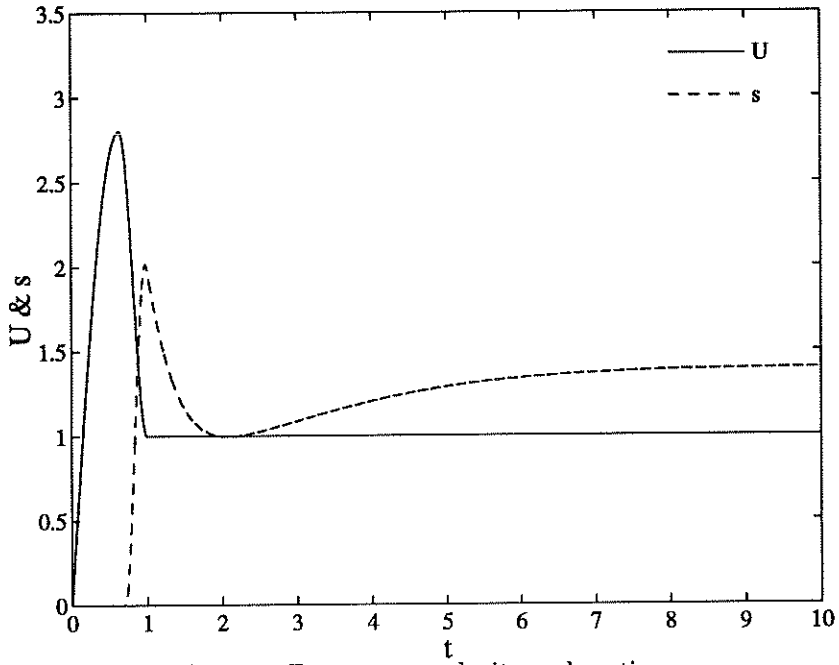

Figure 7: Free-stream velocity and suction.

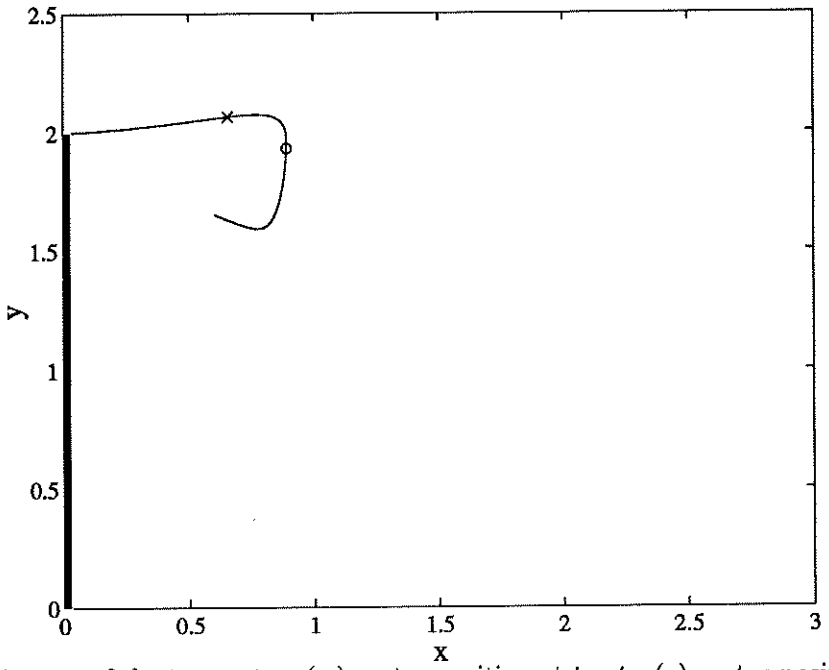

Figure 8: Trajectory of the top vortex, ($\times$) vortex position at $t = t_s$, ($\circ$) vortex position at $t = 1$.

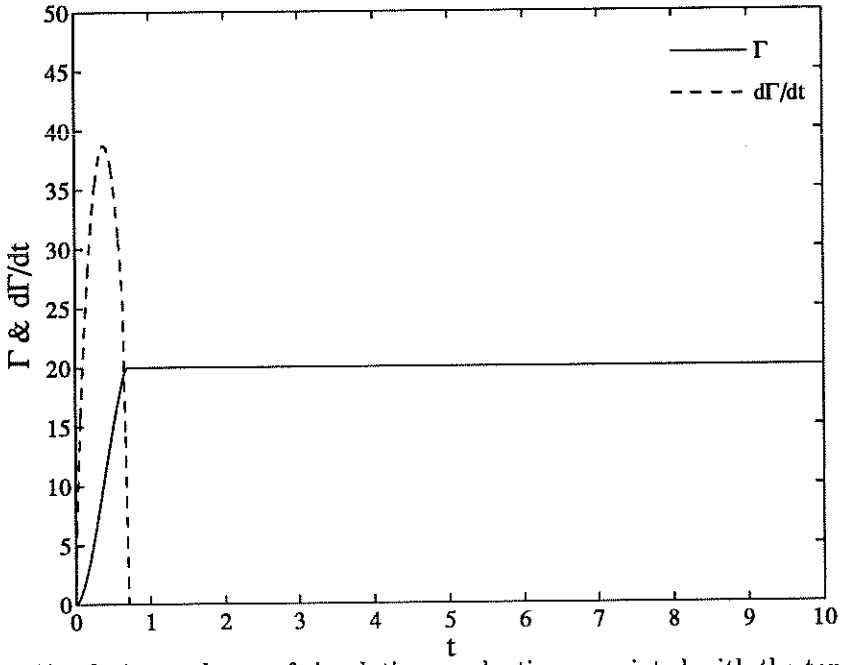

Figure 9: Circulation and rate of circulation production associated with the top vortex.

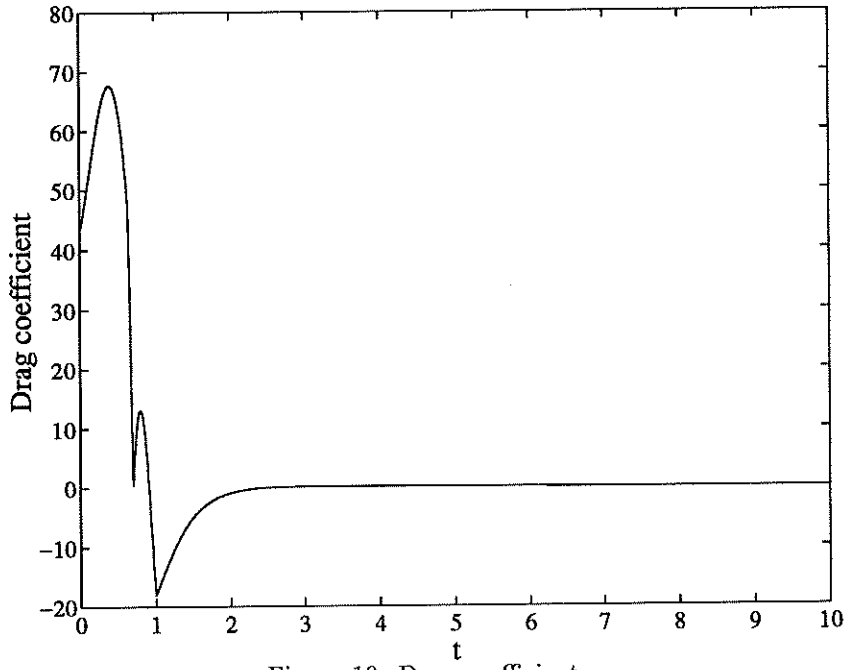

Figure 10: Drag coefficient.

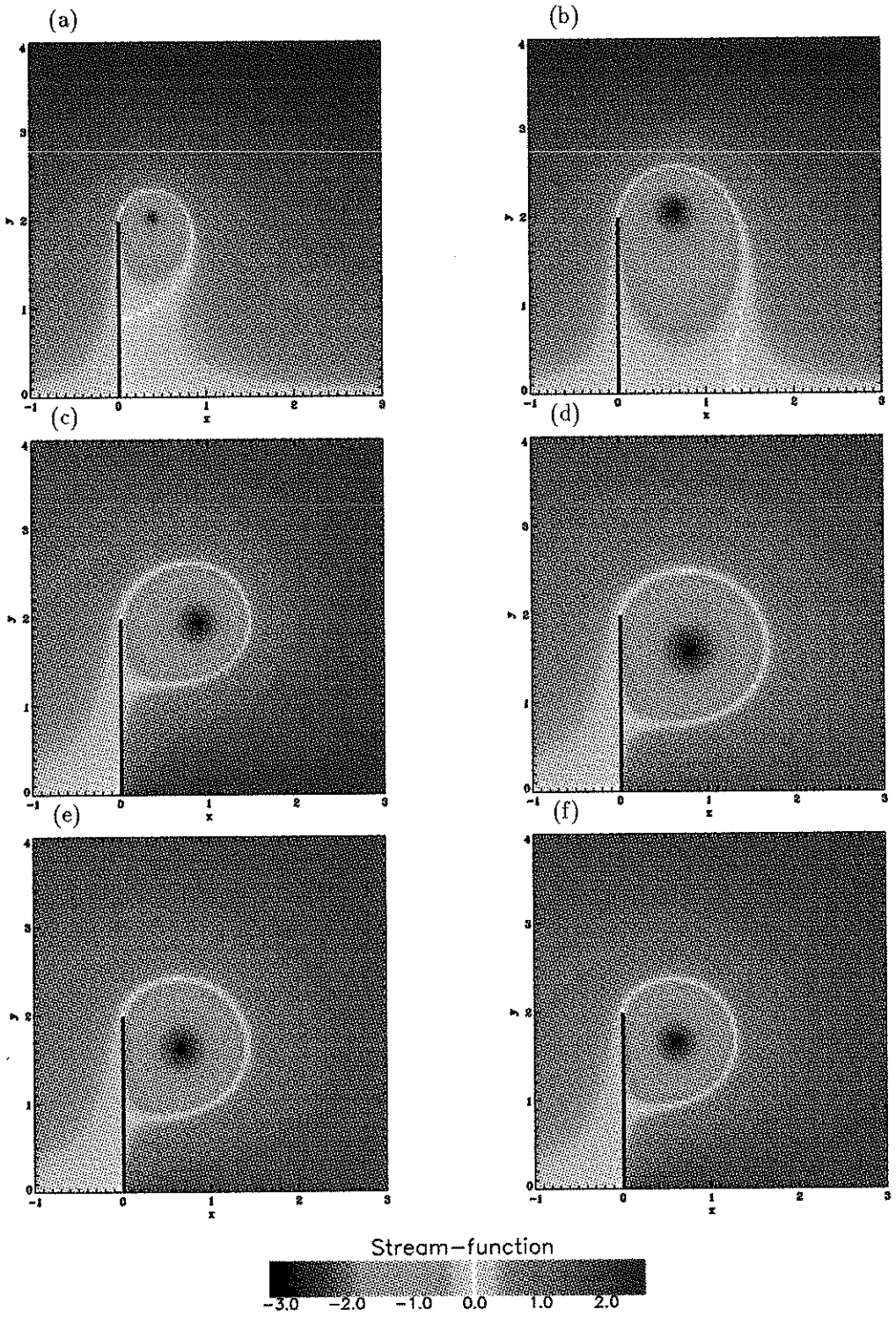

Figure 11: Instantaneous stream-function, t=0.51(a), t=0.71(b), t=1.02(c), t=2.02(d), t=4.02(e), t=8.02(f).

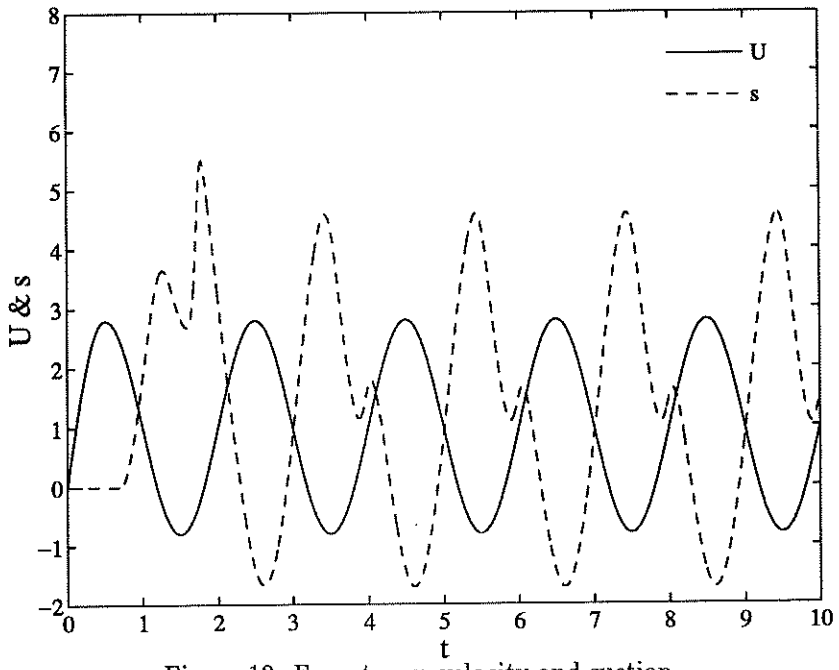

Figure 12: Free-stream velocity and suction.

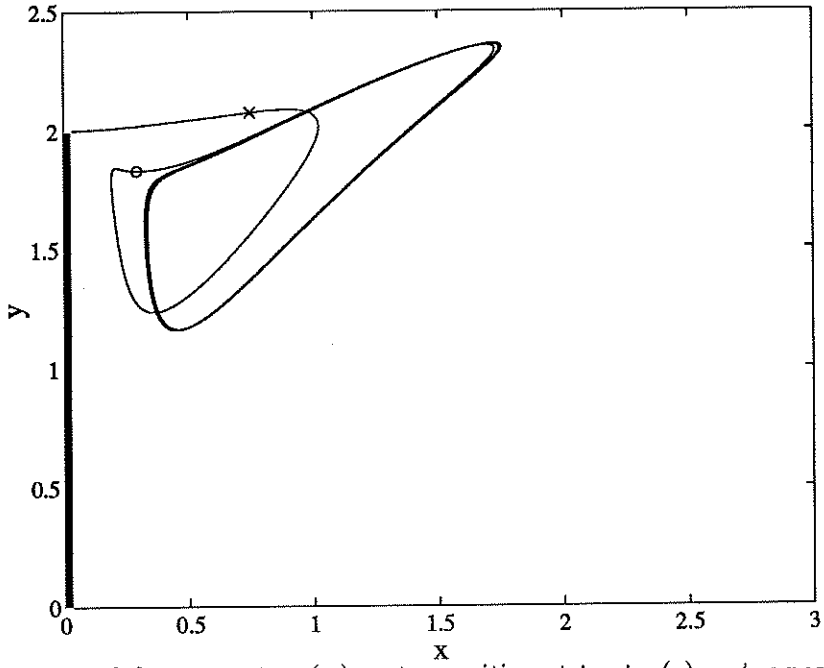

Figure 13: Trajectory of the top vortex, ($\times$) vortex position at $t = t_s$, ($\circ$) vortex position after one period, $t = 2$.

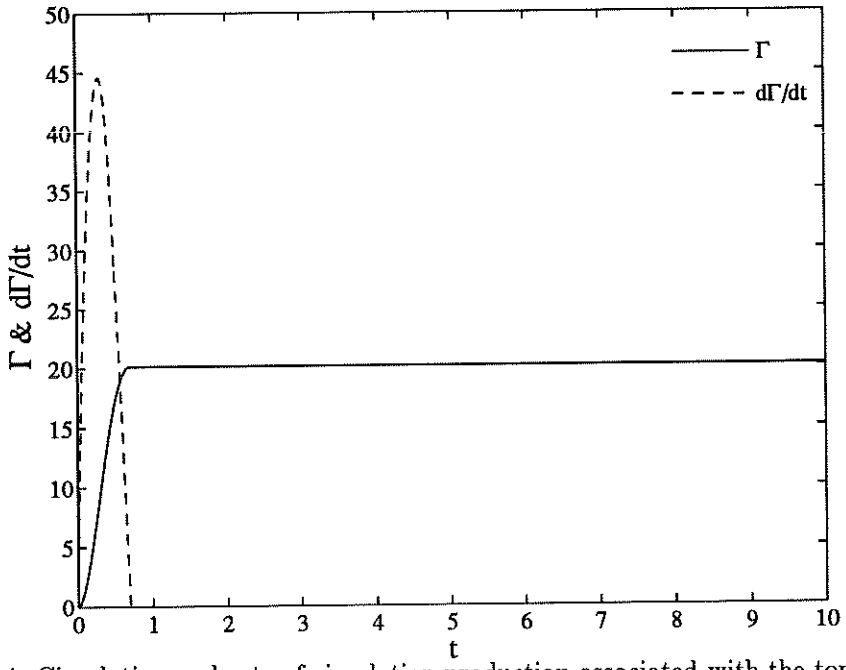

Figure 14: Circulation and rate of circulation production associated with the top vortex.

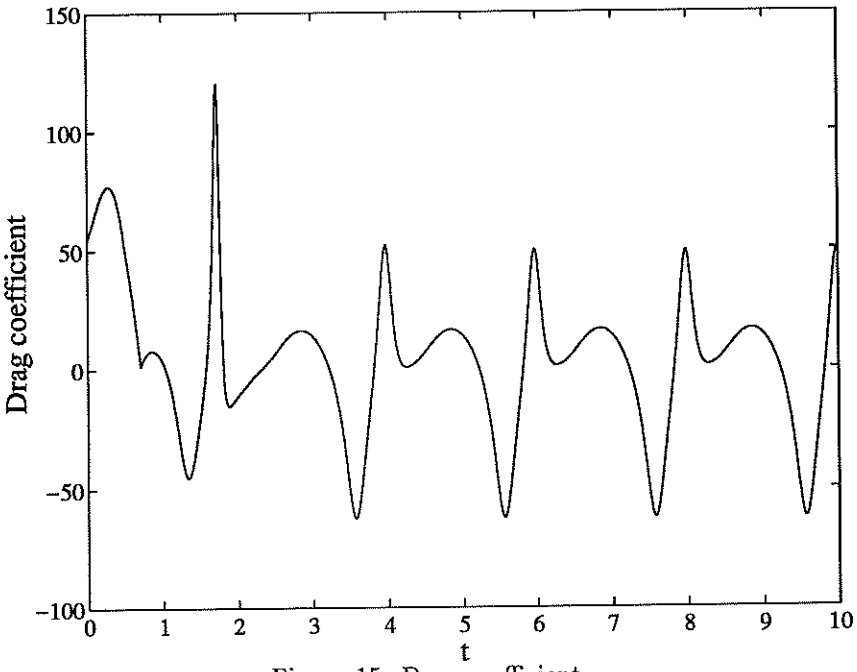

Figure 15: Drag coefficient.

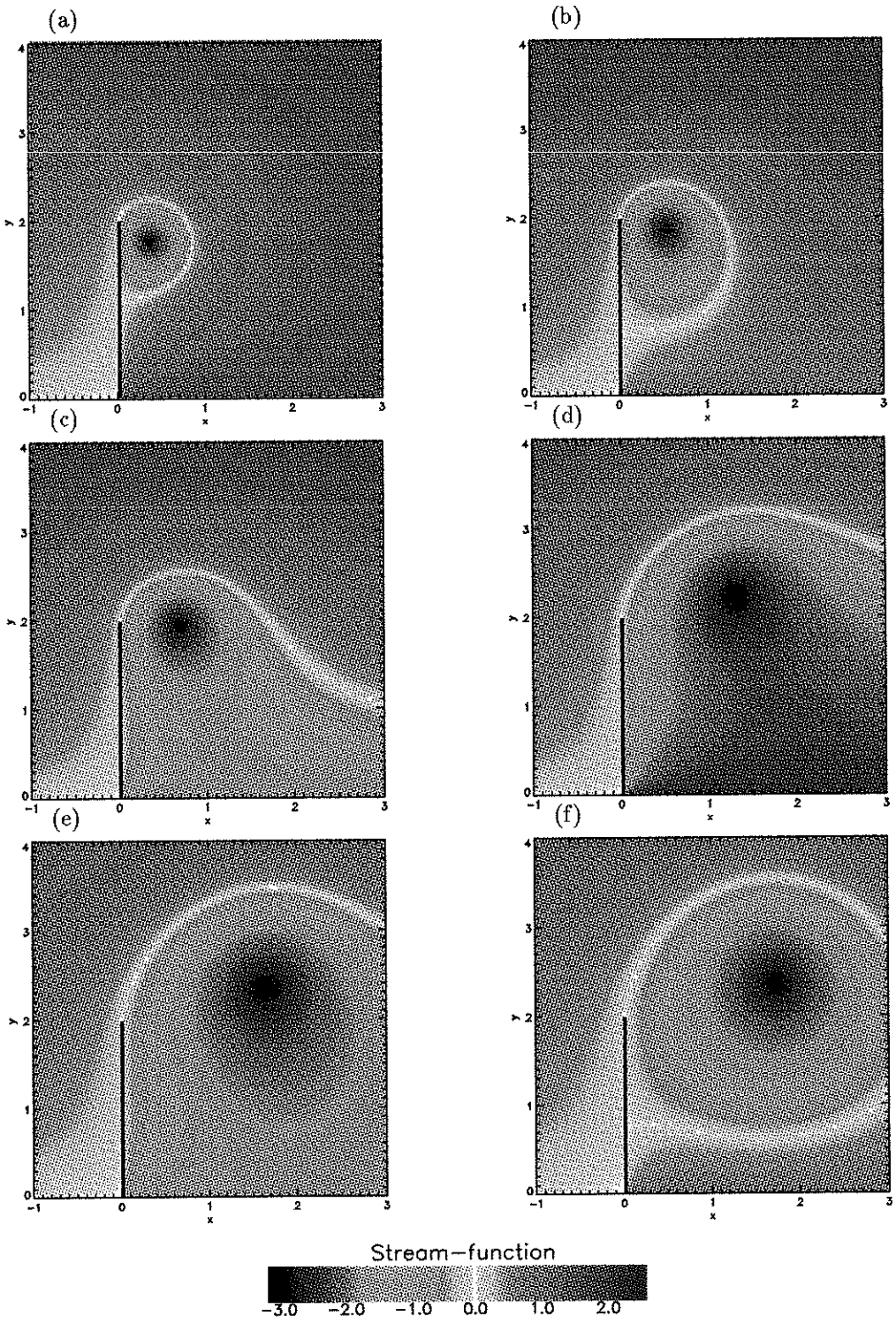

Figure 16: Instantaneous stream-function, t=6.05(a), t=6.25(b), t=6.35(c), t=6.66(d), t=6.86(e), t=6.96(f).

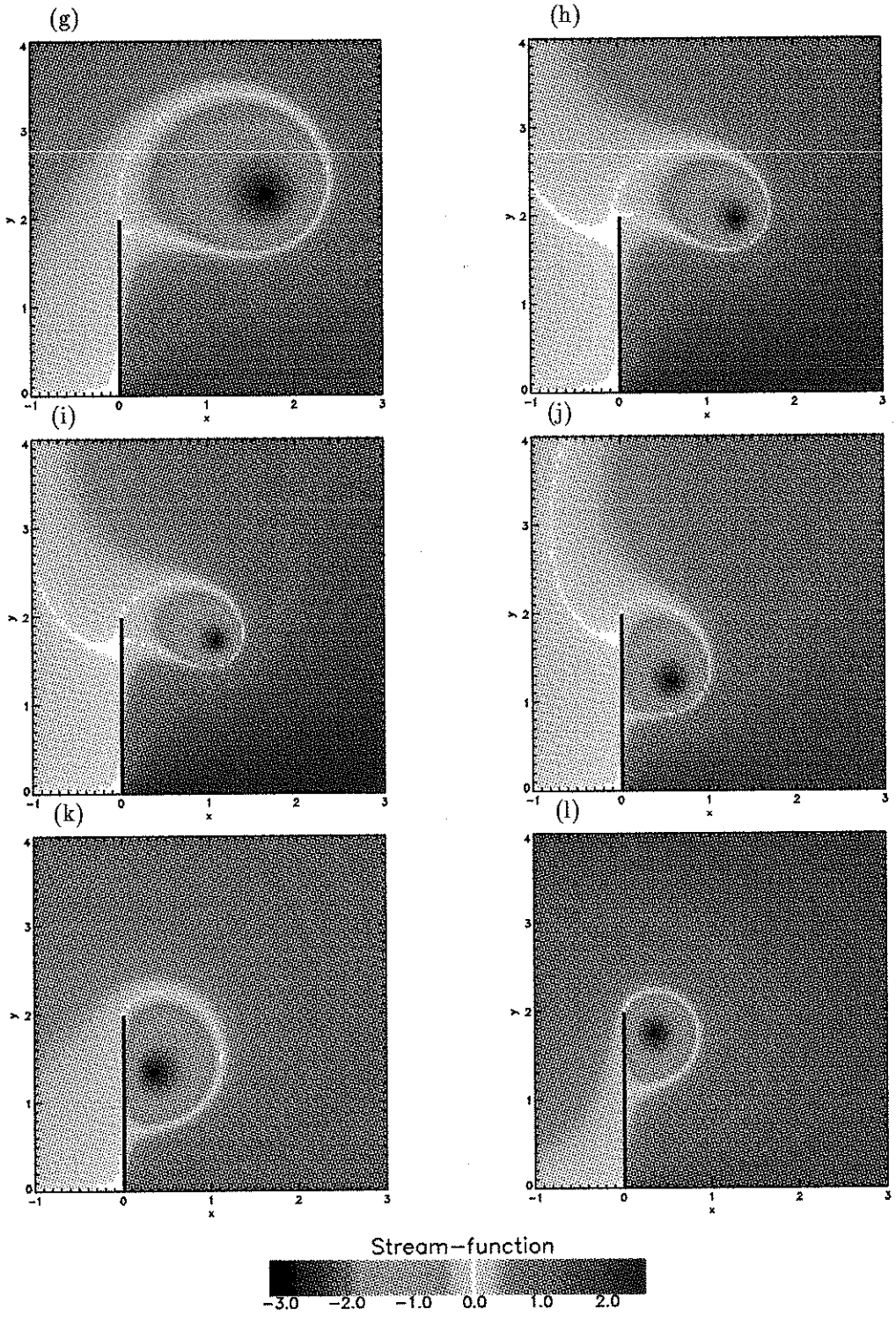

Figure 16: (Continued) Instantaneous stream-function, t=7.16(g), t=7.36(h), t=7.46(i), t=7.67(j), t=7.87(k), t=8.07(l).

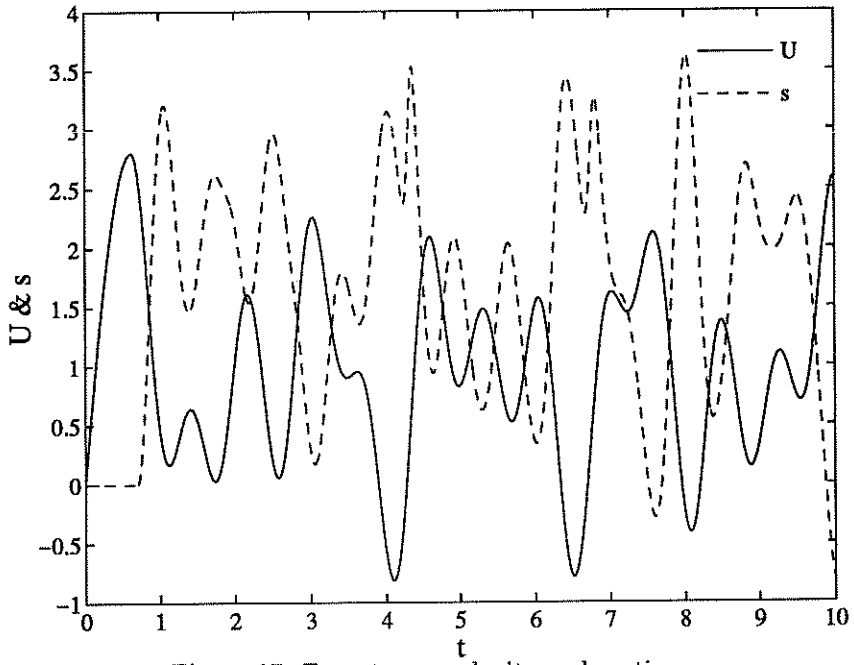

Figure 17: Free-stream velocity and suction.

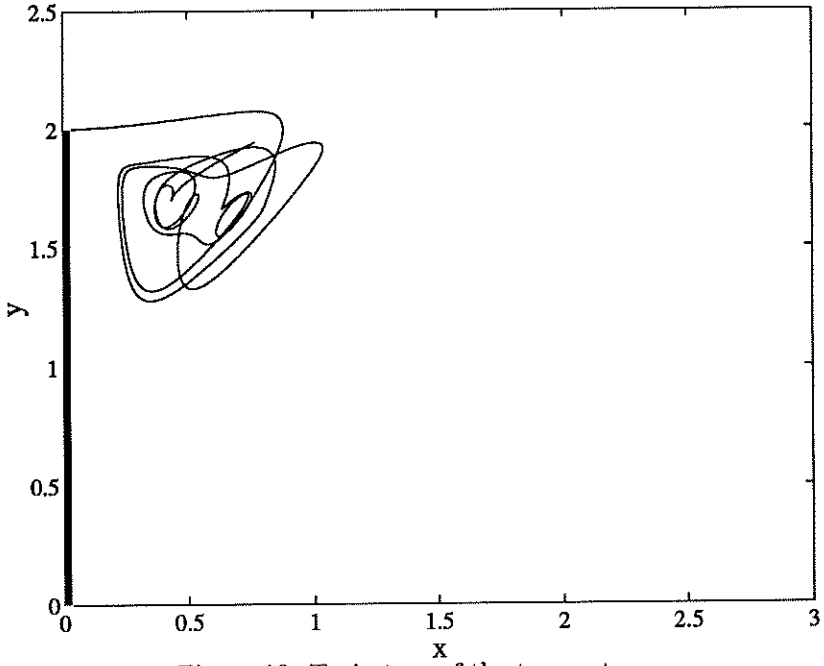

Figure 18: Trajectory of the top vortex.

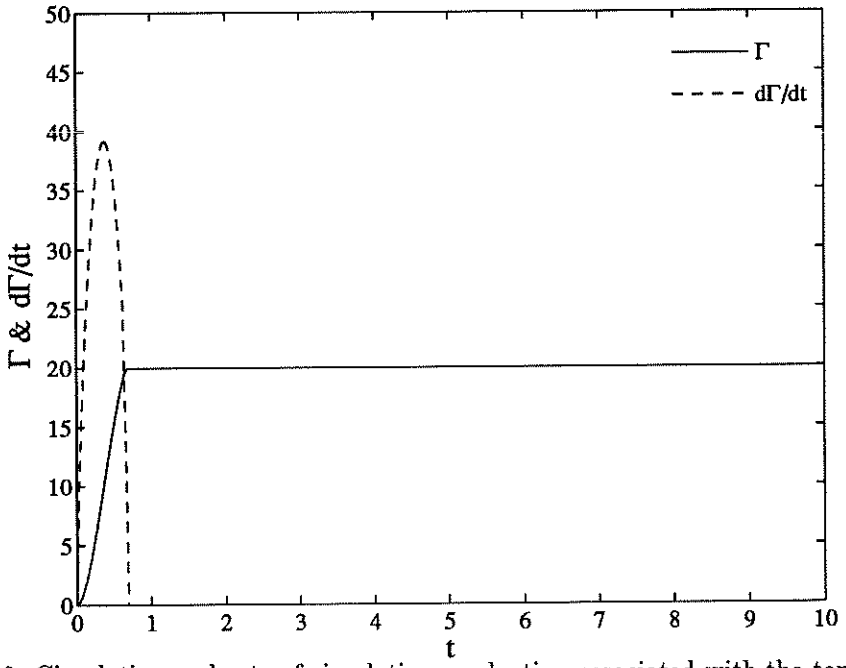

Figure 19: Circulation and rate of circulation production associated with the top vortex.

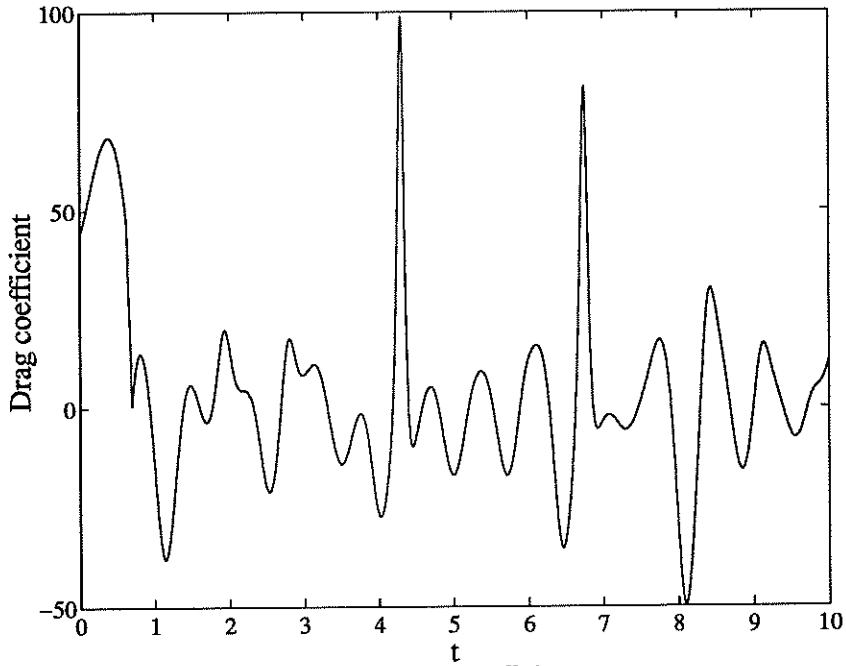

Figure 20: Drag coefficient.

References

Brown, C.E. & Michael, W.H. 1954 Effect of leading-edge separation on the lift of a delta wing. *J. Aero. Sci.* **21**, 690–694.

Cao, N-Z & Aubry, N. 1993 Numerical simulation of a wake flow via a reduced system. FED-Vol. 149, Separated flows, ASME 1993

Cheers, A.Y. 1979 A study of incompressible 2-d vortex flow past a circular cylinder. Lawrence Berkeley Laboratory LBL-9950.

Clements, R.R. 1973 An inviscid model of two-dimensional vortex shedding. *J. Fluid Mech.* **57**, 321–336.

Cortelezzi, L. 1995 Power-law starting flow past a flat plate: Brown and Michael's model, scaling, and universality. University of California at Los Angeles, Report CAM 95-20.

Cortelezzi, L., Leonard, A. & Doyle, J.C. 1994 An example of active circulation control of the unsteady separated flow past a semi-infinite plate. *J. Fluid Mech.* **260**, 127–154.

Doyle, J.C. Francis, B.A. & Tannenbaum, A.R. 1992 Feedback control theory. The Macmillan Company, New York

Fan, M.K.H. Tits, A.L. & Doyle, J.C. 1991 Robustness in the presence of mixed parametric uncertainty and unmodeled dynamics. *IEEE Auto. C.* **36**, 25–38.

Gad-el-Hak, M. & Bushnell, D.M. 1991 Separation control: review. *ASME J. Fluids Eng.* **113**, 5–30.

Graham, J.M.R. 1980 The forces on the sharp-edged cylinders in oscillatory flow at low Keulegan-Carpenter numbers. *J. Fluid Mech.* **97**, 331–346.

Gopalkrishnan, R., Triantafyllou, M.S., Triantafyllou, G.S. & Barrett, D 1994 Active vorticity control in a shear flow using a flapping foil. *J. Fluid Mech.* **274**, 1–21.

Guckenheimer, J. & Holmes, P. 1983 Nonlinear oscillations, dynamical systems, and bifurcation of vector fields. Springer-Verlag, New York

Koochesfahani, M.M. & Dimotakis, P.E. 1988 A cancelation experiment in a forced turbulent shear layer. *First National Fluid Dynamics Congress July 25-28, 1988, Cincinnati, Ohio.* AIAA Paper No. 88-3713-CP.

Lisoski, D.L. 1993 Nominally 2-dimensional flow about a normal flat plate. Ph.D. Thesis, California Institute of Technology.

Ongoren, A. & Rockwell, D. 1988a Flow structure from an oscillating cylinder Part 1. Mechanisms of phase shift and recovery in the near wake. *J. Fluid Mech.* **191**, 197–223.

Ongoren, A. & Rockwell, D. 1988b Flow structure from an oscillating cylinder Part 2. Mode competition in the near wake. *J. Fluid Mech.* **191**, 225–245.

Rajaee, M., Karlsson, S.K.F. & Sirovich, L. 1994 Low-dimensional description of free-shear-flow coherent structures and their dynamical behavior. *J. Fluid Mech.* **258**, 1–29.

Rao, D.M. 1987 Vortical flow management techniques. *Prog. Aerospace Sci.* **24**, 173–224.

Rossow, V.J. 1977 Lift enhancement by an external trapped vortex. *10th Fluid and Plasmadynamics Conference, June 27-29, 1977, Albuquerque, New Mexico.* AIAA Paper No. 77-672.

Roussopoulos, K. 1993 Feedback control of vortex shedding at low Reynolds numbers. *J. Fluid Mech.* **248**, 267–296.

Slomski, J.F. & Coleman, R.M. 1993 Numerical simulation of vortex generation and capture above an airfoil. *31st Aerospace Sciences Meeting and Exhibit, January 11-14, 1993, Reno, Nevada.* AIAA Paper No. 93-864.

Tokumaru, P.T. & Dimotakis, P.E. 1991 Rotary oscillation control of a cylinder wake. *J. Fluid Mech.* **224**, 77–90.